

Theoretical Challenges for a Precision Measurement of the W Mass at Hadron Colliders¹

U. Baur

Department of Physics, State University of New York, Buffalo, New York 14260

Abstract. We discuss the $\mathcal{O}(\alpha)$ electroweak radiative corrections to W and Z boson production and their impact on the measurement of the W mass at hadron colliders. The results of recent improved calculations are presented. We also briefly discuss the $\mathcal{O}(\alpha)$ corrections to Drell-Yan production in the high invariant mass region.

I INTRODUCTION

The Standard Model of electroweak interactions (SM) so far has met all experimental challenges and is now tested at the 0.1% level [1]. However, there is little direct experimental information on the mechanism which generates the masses of the weak gauge bosons. In the SM, spontaneous symmetry breaking is responsible for mass generation. The existence of a Higgs boson is a direct consequence of this mechanism. At present the negative result of direct searches performed at LEP2 imposes a lower bound of $M_H > 107.9$ GeV [2] on the Higgs boson mass. Indirect information on the mass of the Higgs boson can be extracted from the M_H dependence of radiative corrections to the W boson mass, M_W , and the effective weak mixing angle, $\sin^2 \theta_{eff}^{lept}$. Assuming the SM to be valid, a global fit to all available electroweak precision data yields a 95% confidence level upper limit on M_H of 188 GeV [3].

In order to extract more accurate information on M_H from electroweak data, it is very important to measure M_W more precisely. Currently, the W boson mass is known to ± 38 MeV [3] from direct measurements. Further improvement in the W mass uncertainty is expected from this years LEP II

¹⁾ Talk given at the MRST Conference, Rochester, NY, May 8 – 9, 2000, to appear in the Proceedings

data taking, and Run II of the Tevatron [4] which is scheduled to begin in March 2001. The ultimate precision expected for M_W from the combined LEP2 experiments is approximately 35 MeV [5]. At the Tevatron, integrated luminosities of order 2 fb^{-1} are foreseen for Run II, and one expects to measure the W mass with a precision of approximately 40 MeV [4] per experiment and decay channel. Preliminary studies indicate that measuring M_W at the LHC with an with a precision of 25 MeV [6] per experiment and decay channel should be possible, although very challenging.

In order to measure the W boson mass with high precision in a hadron collider environment, it is necessary to fully understand and control higher order QCD and electroweak (EW) corrections to W production. The determination of the W mass in a hadron collider environment requires a simultaneous precision measurement of the Z boson mass, M_Z , and width, Γ_Z . When compared to the value measured at LEP, the two quantities help to accurately determine the energy scale and resolution of the electromagnetic calorimeter, and to constrain the muon momentum resolution [7]. It is therefore also necessary to understand the higher order EW corrections to Z boson production in hadronic collisions.

Accurate predictions for W and Z production which include the complete $\mathcal{O}(\alpha)$ corrections are also needed for a measurement of the W cross section, the W/Z cross section ratio, the determination of the W width, and for extracting $\sin^2 \theta_{eff}^{lept}$ from the forward backward asymmetry in the Z peak region. In addition, precise calculations of the Drell-Yan cross section are needed in searches for new physics beyond the SM, such as hidden extra dimensions or additional Z bosons.

In a previous calculation of the EW radiative corrections to W and Z production, only the final state photonic corrections were correctly included [8]. The sum of the soft and virtual parts was estimated from the inclusive $\mathcal{O}(\alpha^2)$ $W \rightarrow \ell \nu(\gamma)$ and $Z \rightarrow \ell^+ \ell^-(\gamma)$ ($\ell = e, \mu$) width and the hard photon bremsstrahlung contribution. Initial state, interference, and weak contributions to the $\mathcal{O}(\alpha)$ corrections were ignored altogether. The unknown part of the $\mathcal{O}(\alpha)$ EW corrections in Ref. [8], combined with effects of multiple photon emission, have been estimated to contribute a systematic uncertainty of $\delta M_W = 15 - 20$ MeV to the measurement of the W mass in Run I [7]. Clearly, in order to achieve the accuracies envisioned for Run II and the LHC, improved theoretical calculations are required.

Recently, new and more accurate calculations of the $\mathcal{O}(\alpha)$ EW corrections to W [9] and Z boson production in hadronic collisions [10,11] became available. In this talk I present an overview of these calculations. They include most of the contributions which were previously ignored. In Section II I briefly describe the calculation of the $\mathcal{O}(\alpha)$ EW corrections to Z boson and high mass Drell-Yan production. In Section III I summarize the results of Ref. [9]. In Section IV I present a brief summary and outlook.

II ELECTROWEAK CORRECTIONS TO Z BOSON AND HIGH MASS DRELL-YAN PRODUCTION

A The $\mathcal{O}(\alpha)$ QED Corrections to Di-lepton Production

For $p\bar{p} \rightarrow Z, \gamma^* \rightarrow \ell^+\ell^-$, the pure QED corrections form a separately gauge invariant set of diagrams. The first step towards a full calculation of the $\mathcal{O}(\alpha)$ corrections to Z boson production thus consists of performing a calculation of the pure QED corrections. The diagrams contributing to the $\mathcal{O}(\alpha)$ QED corrections can be separated into gauge invariant subsets corresponding to initial and final state corrections.

To perform the calculation, a Monte Carlo method for next-to-leading-order (NLO) calculations similar to that described in Ref. [12] was used. With the Monte Carlo method, it is easy to calculate a variety of observables simultaneously and to simulate detector response. The collinear singularities associated with final state photon radiation are regulated by the mass of the leptons. The associated mass singular logarithms of the form $\log(\hat{s}/m_\ell^2)$, where \hat{s} is the squared parton center of mass energy and m_ℓ is the charged lepton mass, are included in our calculation, but the very small terms of $\mathcal{O}(m_\ell^2/\hat{s})$ are neglected.

The collinear singularities associated with initial state photon radiation can be removed by universal collinear counter terms generated by “renormalizing” the parton distribution functions (PDF’s) [13], in complete analogy to gluon emission in QCD. In addition to the collinear counterterms, finite terms can be absorbed into the PDF’s, introducing a QED factorization scheme dependence. We have carried out our calculation in the QED \overline{DIS} and QED \overline{MS} scheme. In order to treat the $\mathcal{O}(\alpha)$ initial state QED corrections to Z boson production in hadronic collisions in a consistent way, QED corrections should be incorporated in the global fitting of the PDF’s using the same factorization scheme which has been employed to calculate the cross section. Current fits to the PDF’s do not include QED corrections, which introduces a small uncertainty into the calculation.

In Fig. 1a we display the ratio of the $\mathcal{O}(\alpha^3)$ and the Born cross section as a function of the $\ell^+\ell^-$ invariant mass in $p\bar{p} \rightarrow \gamma^*, Z \rightarrow \ell^+\ell^-$ at Tevatron energies. In the region $40 \text{ GeV} < m(\ell^+\ell^-) < 110 \text{ GeV}$, the cross section ratio is seen to vary rapidly. Below the Z peak, QED corrections enhance the cross section by up to a factor 2.7 (1.9) for electrons (muons). The maximum enhancement of the cross section occurs at $m(\ell^+\ell^-) \approx 75 \text{ GeV}$. At the Z peak, the differential cross section is reduced by about 30% (20%). For $m(\ell^+\ell^-) > 130 \text{ GeV}$, the $\mathcal{O}(\alpha)$ QED corrections uniformly reduce the differential cross section by about 12% in the electron case, and $\approx 7\%$ in the muon case.

In Fig. 1b, we compare the impact of the full $\mathcal{O}(\alpha)$ QED corrections (solid line) on the muon pair invariant mass spectrum with that of final

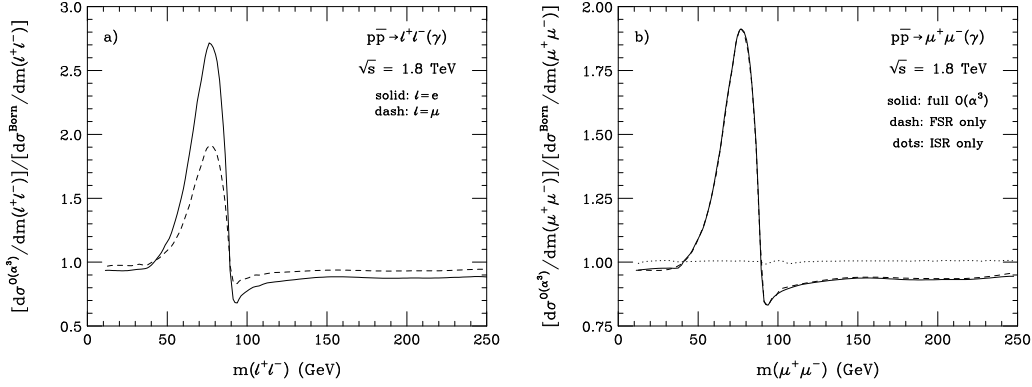


FIGURE 1. Ratio of the $\mathcal{O}(\alpha^3)$ and lowest order differential cross sections as a function of the di-lepton invariant mass for $p\bar{p} \rightarrow \ell^+\ell^-(\gamma)$ at $\sqrt{s} = 1.8$ TeV. Part a) of the figure shows the ratios for electrons and muons in the final state. Part b) shows, for $p\bar{p} \rightarrow \mu^+\mu^-(\gamma)$, the result for the full set of $\mathcal{O}(\alpha^3)$ QED diagrams (solid line), and for taking only final state (dashed line) and initial state corrections (dotted line) into account.

state (dashed line) and initial state radiative corrections (dotted line) only. Qualitatively similar results are obtained in the electron case. Final state radiative corrections are seen to completely dominate over the entire mass range considered. They are responsible for the strong modification of the di-lepton invariant mass distribution. In contrast, initial state corrections are uniform and small ($\approx +0.4\%$).

The results shown in Fig. 1 can be understood by recalling that final state photon radiation leads to corrections which are proportional to $\alpha \log(\hat{s}/m_\ell^2)$. These terms are large, and significantly influence the shape of the di-lepton invariant mass distribution. Photon radiation from one of the leptons lowers the di-lepton invariant mass. Events from the Z peak region therefore are shifted towards smaller values of $m(\ell^+\ell^-)$, thus reducing the cross section in and above the peak region, and increasing the rate below the Z pole. Due to the $\log(\hat{s}/m_\ell^2)$ factor, the effect of the corrections is larger in the electron case.

In Fig. 1, we have not taken into account realistic lepton identification requirements. To simulate detector acceptance, we now impose the following lepton transverse momentum (p_T) and rapidity (η) cuts, which are similar to those used by the CDF Collaboration in Run I:

$$p_T(e) > 20 \text{ GeV}, \quad |\eta(e)| < 2.4, \quad (1)$$

$$p_T(\mu) > 25 \text{ GeV}, \quad |\eta(e)| < 1.0. \quad (2)$$

In addition at least one of the electrons (muons) is required to have $|\eta(e)| < 1.1$ ($|\eta(\mu)| < 0.6$). Uncertainties in the energy measurements of the charged leptons in the detector are simulated in the calculation by Gaussian smearing of the particle four-momentum vector according to the CDF electron and muon

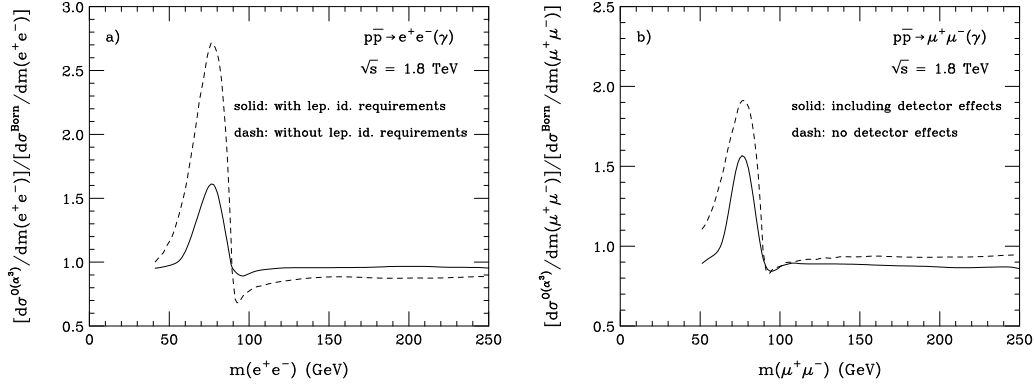


FIGURE 2. Ratio of the $\mathcal{O}(\alpha^3)$ and lowest order differential cross sections as a function of the di-lepton invariant mass for a) $p\bar{p} \rightarrow e^+e^-(\gamma)$ and b) $p\bar{p} \rightarrow \mu^+\mu^-(\gamma)$ at $\sqrt{s} = 1.8$ TeV. The solid (dashed) lines show the cross section ratio with (without) the detector effects described in the text.

momentum resolutions. The granularity of the detector and the size of the electromagnetic showers in the calorimeter make it difficult to discriminate between electrons and photons with a small opening angle. One therefore recombines the four-momentum vectors of the electron and photon to an effective electron four-momentum vector if both traverse the same calorimeter cell. Muons are identified in a hadron collider detector by hits in the muon chambers. In addition, one requires that the associated track is consistent with a minimum ionizing particle. This limits the energy of a photon which traverses the same calorimeter cell as the muon to be smaller than a critical value E_c^γ . In the subsequent discussion, we assume $E_c^\gamma = 2$ GeV.

In Fig. 2a (Fig. 2b) we show how detector effects change the ratio of the $\mathcal{O}(\alpha^3)$ to leading order differential cross sections as a function of the e^+e^- ($\mu^+\mu^-$) invariant mass for $p\bar{p}$ collisions at $\sqrt{s} = 1.8$ TeV. The finite energy resolution and the acceptance cuts have only a small effect on the cross section ratio. The lepton identification criteria, on the other hand, are found to have a large impact. Recombining the electron and photon four-momentum vectors if they traverse the same calorimeter cell eliminates the mass singular terms originating from final state photon radiation. Although the recombination of the electron and photon momenta reduces the effect of the $\mathcal{O}(\alpha)$ QED corrections, the remaining corrections are still sizeable. Below (at) the Z peak, they enhance (suppress) the lowest order e^+e^- differential cross section by up to a factor 1.6 (0.9) (see Fig. 2a). For muon final states (see Fig. 2b), the requirement of $E_\gamma < E_c^\gamma = 2$ GeV for a photon which traverses the same calorimeter cell as the muon reduces the hard photon part of the $\mathcal{O}(\alpha^3)$ $\mu^+\mu^-(\gamma)$ cross section. As a result, the magnitude of the QED corrections below the Z pole is reduced. At the Z pole the corrections remain unchanged,

and for $\mu^+\mu^-$ masses larger than M_Z they become more pronounced.

From Figs. 1 and 2 it is clear that final state bremsstrahlung severely distorts the Breit-Wigner shape of the Z resonance curve. As a result, QED corrections must be included when the Z boson mass is extracted from data, otherwise the mass extracted is shifted to a lower value. In the approximate treatment of the QED corrections to Z boson production used so far by the Tevatron experiments, only final state corrections are taken into account, and the effects of soft and virtual corrections are estimated from the inclusive $\mathcal{O}(\alpha^2)$ $Z \rightarrow \ell^+\ell^-(\gamma)$ width and the hard photon bremsstrahlung contribution [8]. When detector effects are taken into account, the approximate calculation leads to a shift of the Z mass of about -150 MeV in the electron case, and approximately -300 MeV in the muon case [7]. The Z boson mass extracted from the $\ell^+\ell^-$ invariant mass distribution which includes the full $\mathcal{O}(\alpha^3)$ QED corrections is found to be about 10 MeV smaller than that obtained using the approximate calculation of Ref. [8].

The bulk of the shift in M_Z originates from final state photon radiation. This raises the question of how strongly multiple photon radiation influences the measured Z boson mass. An explicit calculation of $\ell^+\ell^-\gamma\gamma$ production in hadronic collisions [14] shows that two photon radiation has a significant impact on the shape of the Z resonance curve. In order to determine its effect on M_Z , more detailed simulations have to be carried out.

B Including Weak Corrections

So far, the purely weak corrections, which mainly consist of vertex corrections and box diagrams with two massive bosons exchanges, were ignored in our discussion. In the Z peak region, these corrections are small. However, at large energies, the effect of the weak vertex and box diagrams becomes large [15]. In this section we present preliminary results of a new calculation [11] which takes into account the purely weak corrections in Z and Drell-Yan production.

In Fig. 3a we show the ratio of the full $\mathcal{O}(\alpha^3)$ electroweak and the $\mathcal{O}(\alpha^3)$ QED differential cross sections for $pp \rightarrow \mu^+\mu^-(\gamma)$ at the LHC as a function of the $\mu^+\mu^-$ invariant mass [6,11]. Here we have imposed a $p_T(\mu) > 20$ GeV and a $|\eta(\mu)| < 3.2$ cut, and used the improved Born approximation (IBA) to evaluate the lowest order contribution to the $\mathcal{O}(\alpha^3)$ QED cross section. Similar results are obtained for the e^+e^- final state and $p\bar{p}$ collisions at Tevatron energies. The IBA incorporates the running electromagnetic coupling constant, the Z propagator expressed in terms of the Fermi constant, G_μ , and the Z boson mass and width measured at LEP, and the vector and axial vector couplings expressed in terms of the effective leptonic weak mixing angle. The ratio shown in Fig. 3a directly displays the effect of the weak box diagrams and the energy dependence of the weak coupling form factors. While the additional

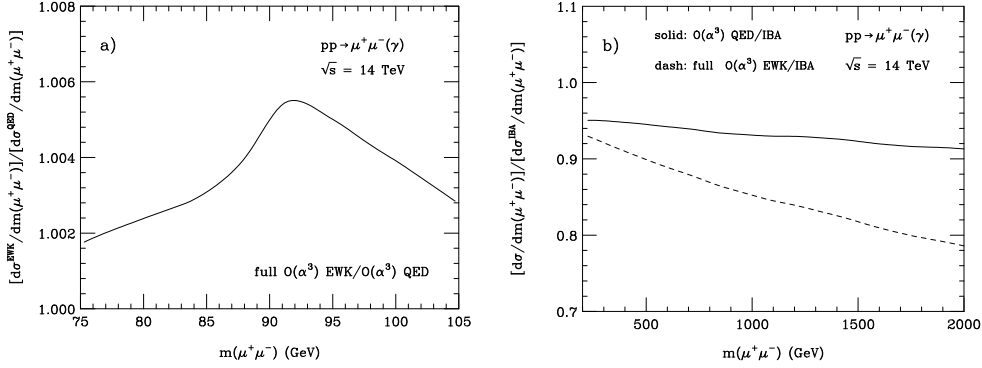


FIGURE 3. a) Ratio of the full $\mathcal{O}(\alpha^3)$ electroweak and the $\mathcal{O}(\alpha^3)$ QED differential cross sections in the vicinity of the Z pole at the LHC. b) Differential cross section ratios at the LHC, displaying the size of the full $\mathcal{O}(\alpha^3)$ electroweak and the $\mathcal{O}(\alpha^3)$ QED corrections for large values of $m(\mu^+ \mu^-)$. The cuts imposed are described in the text.

weak contributions change the differential cross section by 0.6% at most, they do modify the shape of the Z resonance curve.

Figure 3b compares the effect of the $\mathcal{O}(\alpha^3)$ QED corrections and the full $\mathcal{O}(\alpha^3)$ electroweak corrections on the di-muon invariant mass distribution at the LHC for $m(\mu^+ \mu^-)$ values between 200 GeV and 2 TeV. Due to the presence of logarithms of the form $\log(\hat{s}/M_Z^2)$, the weak corrections become significantly larger than the QED corrections at large values of $m(\mu^+ \mu^-)$, and, eventually, may have to be resummed [16]. For $m(\mu^+ \mu^-) = 2$ TeV, the full $\mathcal{O}(\alpha^3)$ electroweak corrections are found to reduce the differential cross section by more than 20%.

III ELECTROWEAK CORRECTIONS TO W BOSON PRODUCTION

The calculation of the $\mathcal{O}(\alpha)$ corrections to W boson production [9] employs the same Monte Carlo method which was used in the Z case. The collinear singularities originating from initial state photon radiation are again removed by counter terms generated by renormalizing the PDF's. Calculating the EW radiative corrections to W boson production, the problem arises how an unstable charged gauge boson can be treated consistently in the framework of perturbation theory. This problem has been studied in Ref. [17] with particular emphasis on finding a gauge invariant decomposition of the EW $\mathcal{O}(\alpha)$ corrections into a QED-like and a modified weak part. In W production, the Feynman diagrams which involve a virtual photon do not represent a gauge invariant subset. In Ref. [17] it was demonstrated how gauge invariant contributions that contain the infrared (IR) singular terms can be extracted

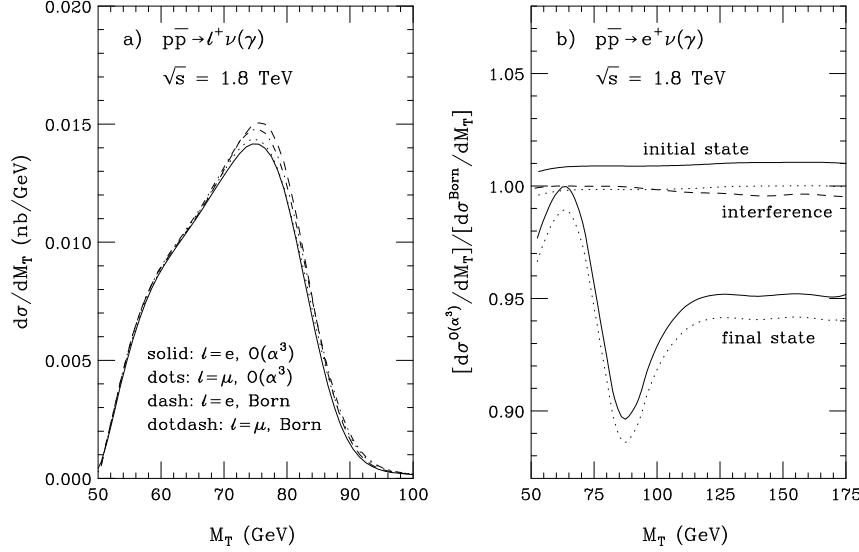


FIGURE 4. a) The M_T distribution for $p\bar{p} \rightarrow \ell^+ \nu(\gamma)$ at $\sqrt{s} = 1.8$ TeV at the Born level and including the EW $\mathcal{O}(\alpha)$ corrections. b) Ratio of the $\mathcal{O}(\alpha^3)$ and lowest order cross sections as a function of the transverse mass for $p\bar{p} \rightarrow e^+ \nu(\gamma)$ at $\sqrt{s} = 1.8$ TeV for various individual contributions. The upper (lower) solid lines show the result for the QED-like initial (final) state corrections. The upper (lower) dotted lines give the cross section ratios if both the QED-like and modified weak initial (final) state corrections are included. The dashed lines display the result if only the initial – final state interference contributions are included.

from the virtual photonic corrections. These contributions can be combined with the also IR-singular real photon corrections in the soft photon region to form IR-finite gauge invariant QED-like contributions corresponding to initial state, final state and interference corrections. The IR finite remainder of the virtual photonic corrections and the pure weak one-loop corrections can be combined to separately gauge invariant modified weak contributions to the W boson production and decay processes.

Since hadron collider detectors cannot directly detect the neutrinos produced in the leptonic W boson decays, $W \rightarrow \ell \nu$, and cannot measure the longitudinal component of the recoil momentum, there is insufficient information to reconstruct the invariant mass of the W boson. Instead, the transverse mass (M_T) distribution of the $\ell \nu$ system, or the p_T distribution of the charged lepton, are used to extract M_W . The M_T distribution for electron and muon final states at the Born level and including $\mathcal{O}(\alpha)$ corrections at the Tevatron is shown in Fig. 4a. The various individual contributions to the EW $\mathcal{O}(\alpha)$ corrections of the M_T distribution in the electron case are shown in Fig. 4b. To model the detector acceptance, the following p_T and η cuts were imposed in Fig. 4:

$$p_T(\ell) > 25 \text{ GeV}, \quad |\eta(\ell)| < 1.2, \quad \ell = e, \mu, \quad (3)$$

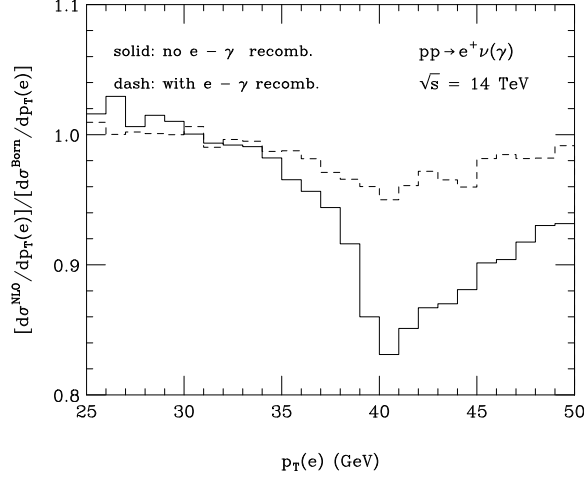


FIGURE 5. Ratio of the $\mathcal{O}(\alpha^3)$ and lowest order $pp \rightarrow e^+ \nu(\gamma)$ differential cross sections at the LHC as a function of the transverse momentum of the electron with and without electron – photon recombination. The cuts imposed are described in the text.

$$\not{p}_T > 25 \text{ GeV.} \quad (4)$$

These cuts are similar to the acceptance cuts used by the DØ collaboration in their W mass analyses in Run I. As before, uncertainties in the energy and momentum measurements of the charged leptons in the detector are simulated in the calculation by Gaussian smearing of the particle four-momentum vector.

The initial state QED-like contribution uniformly increases the cross section by about 1%. It is largely canceled by the modified weak initial state contribution. The interference contribution is very small. It decreases the cross section by about 0.01% for transverse masses below M_W , and by up to 0.5% for $M_T > M_W$. The final state QED-like contribution significantly changes the shape of the transverse mass distribution and reaches its maximum effect in the region of the Jacobian peak, $M_T \approx M_W$. As for the initial state, the modified weak final state contribution reduces the cross section by about 1%, and has no effect on the shape of the transverse mass distribution. Since the final state QED-like contribution is proportional to $\log(\hat{s}/m_\ell^2)$, its size for muons is considerably smaller than for electrons. The initial state corrections and the interference contribution are very similar for electron and muon final states.

In Fig. 4, we have not taken into account the recombination of electrons and photons if their opening angle is small. As in Z boson production, when recombination is included, the mass singular logarithmic terms are eliminated. This significantly reduces the size of the EW corrections. Figure 5 demonstrates the effect for the transverse momentum distribution of the electron in $pp \rightarrow e^+ \nu(\gamma)$ at the LHC. The solid histogram shows the cross section ratio taking only the transverse momentum and pseudorapidity cuts of Eqs. (3) and (4) into account. The dashed histogram displays the result

obtained when in addition the four momentum vectors are smeared according to the ATLAS specifications [18], and electron and photon momenta are combined if $\Delta R(e, \gamma) < 0.07$ [18]. Qualitatively similar results are obtained for Tevatron energies and CDF and DØ lepton identification criteria.

As we have seen, final state bremsstrahlung has a non-negligible effect on the shape of the M_T distribution in the Jacobian peak region. As in the Z boson case, final state photon radiation shifts the W boson mass extracted from data to a lower value. In the approximate treatment of the electroweak corrections used so far by the Tevatron experiments, only final state QED corrections are taken into account; initial state, interference, and weak correction terms are ignored. Furthermore, the effect of the final state soft and virtual photonic corrections is estimated from the inclusive $\mathcal{O}(\alpha^2)$ $W \rightarrow \ell\nu(\gamma)$ width and the hard photon bremsstrahlung contribution [8]. When detector effects are included, the approximate calculation leads to a shift of about -50 MeV in the electron case, and approximately -160 MeV in the muon case [7]. Since only one of the W decay products radiates photons, the shift in M_W is about a factor 2 smaller than the shift in M_Z caused by photon radiation.

Initial state and interference contributions do not change the shape of the M_T distribution significantly (see Fig. 4b) and therefore have little effect on the extracted mass. However, correctly incorporating the final state virtual and soft photonic corrections results in a non-negligible modification of the shape of the transverse mass distribution for $M_T > M_W$. For W production at the Tevatron this is demonstrated in Fig. 6, which shows the ratio of the M_T distribution obtained with the QED-like final state correction part of our calculation to the one obtained using the approximation of Ref. [8].

The difference in the line shape of the M_T distribution between the $\mathcal{O}(\alpha^3)$ calculation of Ref. [9] and the approximation used so far occurs in a region which is important for both the determination of the W mass, and the direct measurement of the W width. The precision which can be achieved in a measurement of M_W using the transverse mass distribution strongly depends on how steeply the M_T distribution falls in the region $M_T \approx M_W$. Any change in the theoretical prediction of the line shape thus directly influences the W mass measurement. From a maximum likelihood analysis the shift in the measured W mass due to the correct treatment of the final state virtual and soft photonic corrections is found to be $\Delta M_W \approx \mathcal{O}(10 \text{ MeV})$. For the precision expected in Run II and for the LHC such a shift cannot be ignored.

Two photon radiation has only a modest effect on the shape of the M_T distribution [14]. Detailed simulations will be necessary to determine its effect on the W mass.

The calculation presented in Ref. [9] was carried out in the pole approximation, ie. the form factors associated with the modified weak corrections were evaluated at $\hat{s} = M_W^2$. This approximation is valid in the vicinity of the W pole. Away from the resonance region it will be important to go beyond the pole approximation. Calculations which do so are in progress [19]. Preliminary

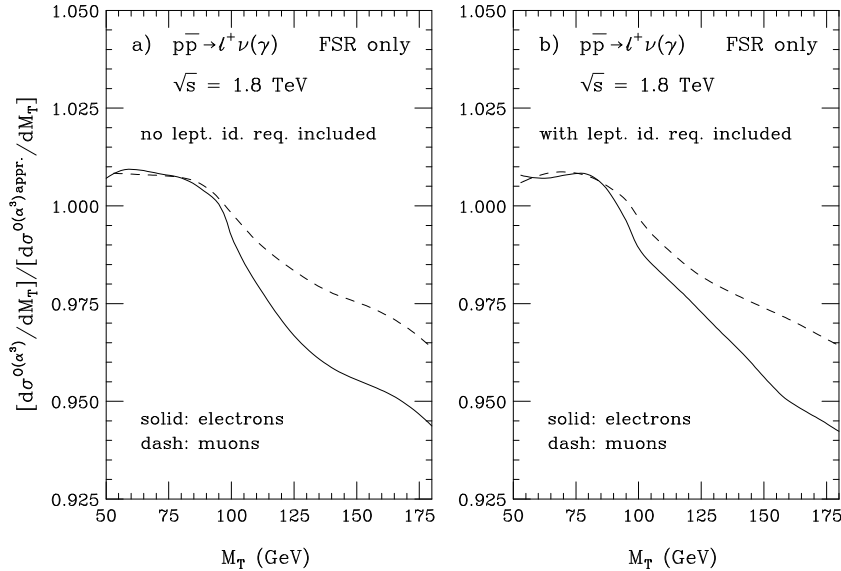


FIGURE 6. Ratio of the M_T distributions obtained with the QED-like final state correction part of Ref. [10] to the one obtained using the approximation of Ref. [8] for $p\bar{p} \rightarrow \ell^+ \nu(\gamma)$ at $\sqrt{s} = 1.8$ TeV.

results [6] indicate that the radiative corrections for $p_T(\ell) > 200$ GeV in a full calculation are up to a factor 2 larger than those calculated in the pole approximation. This may be important for a measurement of the W width from the high transverse mass tail.

IV SUMMARY AND OUTLOOK

Accurate theoretical predictions for W and Z boson production are essential for many important electroweak precision measurements in future hadron collider experiments, in particular the measurement of the W mass and width. In addition, comparison of the Z boson mass and width with the values obtained at LEP will help to calibrate detectors. All these measurements require a detailed understanding of the EW radiative corrections. I have described the current status of calculations of the $\mathcal{O}(\alpha)$ EW corrections to W and Z boson production in hadronic collisions. These calculations will be complete by the time Run II of the Tevatron is expected to start. Much more work is required to determine the effect of multiple photon radiation on the weak boson masses extracted from hadron collider experiments.

ACKNOWLEDGEMENTS

This work has been supported by NSF grant PHY-9970703.

REFERENCES

1. D. Abbaneo *et al.* (The LEP Electroweak Working Group), CERN-EP-2000-016 (January 2000).
2. P. Bock *et al.* (The LEP Working Group on Higgs Boson searches), CERN-EP-2000-055 (April 2000).
3. A. Straessner, talk given at the XXXVth Rencontres de Moriond, “Electroweak Interactions and Unified Theories”, 11 – 18 March 2000, Les Arcs, France.
4. H. Aihara *et al.*, in “Future Electroweak Physics at the Fermilab Tevatron: Report of the TEV_2000 Study Group”, edited by D. Amidei and R. Brock, Fermilab-Pub-96/082, 1996, p. 63.
5. D.G. Charlton, hep-ex/9912019, To be published in the proceedings of the “19th International Symposium on Lepton and Photon Interactions at High-Energies”, Stanford, California, 9 – 14 August 1999.
6. S. Haywood *et al.*, hep-ph/0003275, Proceedings of the “1999 CERN Workshop on Standard Model Physics (and more) at the LHC”, CERN Yellow Report CERN-2000-004, eds. G. Altarelli and M. Mangano.
7. F. Abe *et al.* (CDF Collaboration), Phys. Rev. Lett. **75**, 11 (1995) and Phys. Rev. **D52**, 4784 (1995); T. Affolder *et al.* (CDF Collaboration), hep-ex/0007044 (July 2000); S. Abachi *et al.* (DØ Collaboration), Phys. Rev. Lett. **77**, 3309 (1996); B. Abbott *et al.* (DØ Collaboration), Phys. Rev. **D58**, 012002 (1998), Phys. Rev. **D58**, 092003 (1998) and Phys. Rev. Lett. **80**, 3008 (1998).
8. F.A. Berends and R. Kleiss, Z. Phys. **C27**, 365 (1985).
9. U. Baur, S. Keller and D. Wackeroth, Phys. Rev. **D59**, 013002 (1999).
10. U. Baur, S. Keller and W.K. Sakumoto, Phys. Rev. **D57**, 199 (1998).
11. U. Baur, O. Brein, W. Hollik, C. Schappacher and D. Wackeroth, in preparation.
12. H. Baer, J. Ohnemus, and J.F. Owens, Phys. Rev. **D40**, 2844 (1989); W. Giele and E.W.N. Glover, Phys. Rev. **D46**, 198 (1992).
13. J. Kripfganz and H. Perl, Z. Phys. **C41**, 319 (1988); H. Spiesberger, Phys. Rev. **D52**, 4936 (1995); A. de Rujula *et al.*, Nucl. Phys. **B154**, 394 (1979).
14. U. Baur and T. Stelzer, Phys. Rev. **D61**, 073007 (2000).
15. P. Ciafaloni and D. Comelli, Phys. Lett. **B446**, 278 (1999).
16. J. H. Kühn and A. A. Penin, hep-ph/9906545; J.H. Kühn, A.A. Penin and V.A. Smirnov, hep-ph/9912503 and hep-ph/0005301; V. S. Fadin, L. N. Lipatov, A. D. Martin and M. Melles, Phys. Rev. **D61**, 094002 (2000); M. Melles, hep-ph/0004056 and hep-ph/0006077; W. Beenakker and A. Werthenbach, hep-ph/0005316.
17. W. Hollik and D. Wackeroth, Phys. Rev. **D55**, 6788 (1997).
18. ATLAS Collaboration, “ATLAS Detector and Physics Performance”, CERN/LHCC/99-15 (1999).
19. U. Baur and D. Wackeroth, in preparation; S. Dittmaier and M. Krämer, in preparation.